J. Fluid Mech. (2007), *vol.* 587, *pp.* 163–172. © 2007 Cambridge University Press
doi:10.1017/S0022112007007549 Printed in the United Kingdom

Motion of a sphere normal to a wall in a second-order fluid

A. M. ARDEKANI[1], R. H. RANGEL[1] AND D. D. JOSEPH[1,2]

[1]Department of Mechanical and Aerospace Engineering, University of California, Irvine, CA 92697-3975, USA

[2]Department of Aerospace Engineering and Mechanics, University of Minnesota, MN 55455, USA

(Received 3 April 2007 and in revised form 1 July 2007)

The motion of a sphere normal to a wall is investigated. The normal stress at the surface of the sphere is calculated and the viscoelastic effects on the normal stress for different separation distances are analysed. For small separation distances, when the particle is moving away from the wall, a tensile normal stress exists at the trailing edge if the fluid is Newtonian, while for a second-order fluid a larger tensile stress is observed. When the particle is moving towards the wall, the stress is compressive at the leading edge for a Newtonian fluid whereas a large tensile stress is observed for a second-order fluid. The contribution of the second-order fluid to the overall force applied to the particle is towards the wall in both situations. Results are obtained using Stokes equations when $\alpha_1 + \alpha_2 = 0$. In addition, a perturbation method has been utilized for a sphere very close to a wall and the effect of non-zero $\alpha_1 + \alpha_2$ is discussed. Finally, viscoelastic potential flow is used and the results are compared with the other methods.

1. Introduction

Expansion of the general stress function for slow and slowly varying motion gives rise to the second-order fluid which is introduced by Coleman & Noll (1960) (see also Rivlin & Ericksen 1995; Bird, Armstrong & Hassagner 1987; Joseph 1990). Correct predictions have been obtained for second-order fluids for the orientation of a settling long body, the evolution of the Jeffery orbit (Leal 1975) and the lateral migration of a sphere in a non-homogeneous shear flow (Ho & Leal 1976). However, the predictions of the fluid response to rapid motions have not been satisfactory.

The motion of bodies in viscoelastic fluids is completely different form that in a Newtonian fluid. The broadside of a long body sedimenting in a Newtonian fluid is perpendicular to the stream, which is due to inertia and is usually explained by turning couples at the stagnation points. However the broad-side aligns parallel to the stream in a viscoelastic fluid (Liu & Joseph 1993). Wang & Joseph (2004) have utilized viscoelastic potential flow for second-order fluid around an ellipse. They calculated the normal stress at the stagnation points of an ellipse and showed that turning couples in the second-order fluid can be explained by calculating the moments on the ellipse. Particle–particle interaction can be described as drafting, kissing and tumbling in Newtonian fluid for non-zero-Reynolds-number flows (Fortes, Joseph & Lundgren 1987) while for Stokes flows, the particle configuration remains unchanged as the particles sediment (Ardekani & Rangel 2006). In contrast, if two spheres are set into motion in a viscoelastic fluid in an initial side-by-side configuration in which

the two spheres are separated by a smaller than critical gap, the spheres will attract, turn and chain in the direction parallel to the stream. This can be explained by looking at the normal stresses at the points of stagnation on the spheres, which are compressive in Newtonian fluids and tensile in viscoelastic fluids (Wang & Joseph 2004). The cusped trailing edge of an air bubble rising in viscoelastic fluid can also be qualitatively explained by examining normal stresses on the surface of the bubble predicted by viscoelastic potential flow. In this paper, we study the effect of the second-order fluid on the normal stresses and forces acting on a particle moving normal to a wall.

This study is important in understanding particle–wall collision, which has been investigated for Newtonian fluids by several researchers (Davis 1987; Joseph *et al.* 2001; Ardekani & Rangel 2007) not but apparently addressed in the context of viscoelastic fluids. Understanding the particle–wall interaction in viscoelastic fluids facilitates the study of collision processes. Small particles moving in such fluids near walls occur in applications such as separation techniques, biological flows, sediment transport, and the falling-sphere viscometer. The extension of the results presented here to binary interactions of particles can be used in the calculation of properties of a suspension of particles in second-order fluids. Sedimentation velocities, bulk stresses, etc. for suspension of spheres in Newtonian fluids have been studied by several researchers (e.g. Batchelor & Green 1972 and Jeffrey 1973). However, few studies have discussed the stress in dilute suspension of spheres in second-order fluid (Mifflin 1985; Sun & Jayaraman 1984; Koch & Subramanian 2006). An alternative to the implementation in the present study would be twin method of expansion used by Jeffrey (1973).

The interaction between a sphere and a vertical wall has been extensively studied experimentally and numerically (Goldman, Cox & Brenner 1967; Joseph *et al.*, 1994; Becker, McKinley & Stone 1996; Singh & Joseph 2000). As these studies show, a sedimenting particle is attracted to a vertical wall in viscoelastic fluids. Rodin (1995) considered the squeezing of a film between two spheres in a power-law fluid using asymptotic solutions. Viscoelastic squeezed films are also considered by Brindley, Davies & Walters (1976) and Engmann, Servais & Burbidge (2005). Riddle, Narvaez & Bird (1977) experimentally investigated the distance between two identical spheres falling along their line of centers in viscoelastic fluids. They found that the spheres attract if they are initially close and separate if they are not close. Brunn (1977) considered the interaction of two identical spheres sedimenting in a quiescent second-order fluid and observed that the distance between spheres decreases as they fall. His analysis applies when the particle separation is large and he did not find a critical separation distance for attraction. In this study, the motion of a spherical particle perpendicularly to a wall in a second-order fluid is studied and the results obtained by Stokes analysis are compared with those from a perturbation method and using viscoelastic potential flow.

2. Theoretical development

The governing equations for a second-order fluid are as follows:

$$\rho\left[\frac{\partial \boldsymbol{u}}{\partial t}+(\boldsymbol{u}\cdot\nabla)\boldsymbol{u}\right]=\nabla\cdot\boldsymbol{T}, \qquad \nabla\cdot\boldsymbol{u}=0, \tag{2.1}$$

where $\boldsymbol{u}$ is the velocity field and ρ is the fluid density. The stress tensor $\boldsymbol{T}$ for an incompressible second-order fluid is

$$\boldsymbol{T} = -p\boldsymbol{I} + \mu_f \boldsymbol{A} + \alpha_1 \boldsymbol{B} + \alpha_2 \boldsymbol{A}^2, \tag{2.2}$$

where p is the pressure, μ_f is the zero shear viscosity, $\boldsymbol{A} = \nabla\boldsymbol{u} + \nabla\boldsymbol{u}^T$ is twice the symmetric part of the velocity gradient and

$$\boldsymbol{B} = \frac{\partial \boldsymbol{A}}{\partial t} + (\boldsymbol{u}\cdot\nabla)\boldsymbol{A} + \boldsymbol{A}\nabla\boldsymbol{u} + \nabla\boldsymbol{u}^T\boldsymbol{A}; \tag{2.3}$$

$\alpha_1 = -\frac{1}{2}\psi_1$ and $\alpha_2 = \psi_1 + \psi_2$ where ψ_1 and ψ_2 are the first and second normal stress coefficients.

3. Low-Reynolds-number results

In this study, a spherical particle moving normal to a wall with constant velocity is considered. For low-Reynolds-number flows, in two dimensions or when $\alpha_1 + \alpha_2 = 0$, the velocity field for a second-order fluid is the same as the one predicted by the Stokes flow while pressure becomes

$$p = p_N + \frac{\alpha_1}{\mu_f}\frac{\mathrm{D}p_N}{\mathrm{D}t} + \frac{\beta}{4}\mathrm{tr}\boldsymbol{A}^2, \tag{3.1}$$

where $\beta = 3\alpha_1 + 2\alpha_2$ is the climbing constant and p_N is the Stokes pressure. In this case, the nonlinearities in the constitutive equation affect only the distribution of normal stress (Tanner 1985). $\alpha_1 + \alpha_2$ is positive for the fluids known to us and for simplification this constraint is applied to the fluid in this section. However, different methods are utilized in the following sections and the constraint on normal stress coefficients is removed.

The boundary conditions on the surface of the spheres are more easily expressed in terms of bispherical coordinates. Cylindrical coordinates can be transformed to bispherical coordinates as

$$r = \tilde{c}\frac{\sin\eta}{\cosh\xi - \cos\eta}, \qquad z = \tilde{c}\frac{\sinh\xi}{\cosh\xi - \cos\eta}, \tag{3.2}$$

where the surface of the sphere is at $\xi = \alpha$, $\cosh\alpha = h/a$, $\tilde{c} = a\sinh\alpha$, h is the distance between the particle and the wall and a is the particle radius. Let $\mu = \cos\eta$, then velocity gradient $\nabla\mathbf{u}$ in bispherical coordinates can be written as

$$\nabla\mathbf{u}|_{\text{on particle}} = \frac{\cosh\xi - \mu}{\tilde{c}} \times \begin{pmatrix} \dfrac{\partial u_\xi}{\partial\xi} - u_\eta\dfrac{\sin\eta}{\cosh\xi-\mu} & \dfrac{\partial u_\xi}{\partial\eta} + u_\eta\dfrac{\sinh\xi}{\cosh\xi-\mu} & 0 \\ \dfrac{\partial u_\eta}{\partial\xi} + u_\xi\dfrac{\sin\eta}{\cosh\xi-\mu} & \dfrac{\partial u_\eta}{\partial\eta} - u_\xi\dfrac{\sinh\xi}{\cosh\xi-\mu} & 0 \\ 0 & 0 & \dfrac{-u_\xi\sin\eta\sinh\xi + u_\eta(\mu\cosh\xi - 1)}{\sin\eta(\cosh\xi-\mu)} \end{pmatrix} \tag{3.3}$$

The axisymmetric motion of a sphere towards a wall in Stokes flow has been studied by Brenner (1961) and Maude (1961). Here we briefly summarize the results.

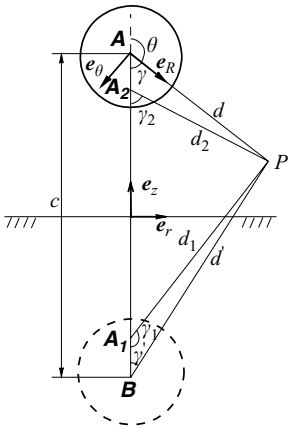

FIGURE 1. A spherical particle moving perpendicular to a wall.

The stream function can be written as

$$\psi = (\cosh\xi - \mu)^{-3/2} \sum_{n=1}^{\infty} U X_n \left(P_{n-1}(\mu) - P_{n+1}(\mu)\right), \tag{3.4}$$

where U is the velocity of the particle $P_n(\mu)$ is the Legendre polynomial of degree n and

$$X_n = \hat{A}_n \cosh\left(n - \frac{1}{2}\right)\xi + \hat{B}_n \sinh\left(n - \frac{1}{2}\right)\xi + \hat{C}_n \cosh\left(n + \frac{3}{2}\right)\xi + \hat{D}_n \sinh\left(n + \frac{3}{2}\right)\xi. \tag{3.5}$$

The coefficients $\hat{A}_n$–$\hat{D}_n$ are described by Brenner (1961). The pressure P_N can be expressed as an infinite summation of spherical harmonics (Pasol *et al.* 2005):

$$p_N = \frac{\mu_f}{\tilde{c}^3}(\cosh\xi - \mu)^{(1/2)} \sum_{n=0}^{\infty} \left[A_n \cosh\left(n + \frac{1}{2}\right)\xi + B_n \sinh\left(n + \frac{1}{2}\right)\xi\right] P_n(\mu). \tag{3.6}$$

The coefficients A_n and B_n are defined by Pasol *et al.* (2005). Calculating u_ξ, u_η, and P_N and using (2.2) and (2.3) the stress tensor in bispherical coordinates ($\boldsymbol{T}_b$) can be calculated. Using the rotation matrix from cylindrical to bispherical coordinates we have

$$\boldsymbol{R}_1 = \begin{pmatrix} \dfrac{\cosh\xi - \mu}{\tilde{c}}\dfrac{\partial r}{\partial \xi} & \dfrac{\cosh\xi - \mu}{\tilde{c}}\dfrac{\partial z}{\partial \xi} & 0 \\ \dfrac{\cosh\xi - \mu}{\tilde{c}}\dfrac{\partial r}{\partial \eta} & \dfrac{\cosh\xi - \mu}{\tilde{c}}\dfrac{\partial z}{\partial \eta} & 0 \\ 0 & 0 & 1 \end{pmatrix}, \qquad \boldsymbol{T}_{cyl} = \boldsymbol{R}_1^T \boldsymbol{T}_b \boldsymbol{R}_1. \tag{3.7}$$

To calculate the stress tensor in spherical coordinates centred at the sphere center, we have

$$\boldsymbol{R}_2 = \begin{pmatrix} \sin\theta & \cos\theta & 0 \\ \cos\theta & -\sin\theta & 0 \\ 0 & 0 & 1 \end{pmatrix}, \qquad \boldsymbol{T}_{sph} = \boldsymbol{R}_2^T \boldsymbol{T}_{cyl} \boldsymbol{R}_2, \tag{3.8}$$

where θ is the polar angle as shown in figure 1. Figure 2(a) shows the dimensionless normal stress as a function of θ for different separation distances when the particle is moving away

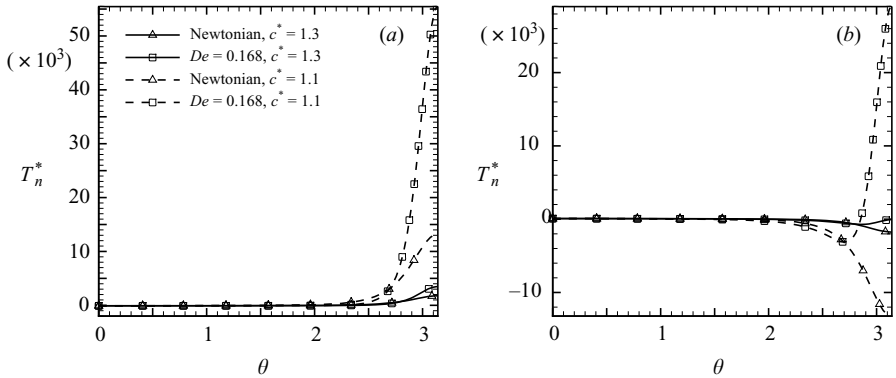

FIGURE 2. A spherical particle moving normal to a wall at $Re = 0.05$, $De = 0.168$: (*a*) away from the wall; (*b*) towards the wall.

from the wall. The stress is non-dimensionalized by $1/2\rho U^2$ and $c^* = c/(2a) = h/a$. Results for low Reynolds and Deborah numbers are shown ($Re = 0.05$ and $De = |\alpha_1 U|/(\mu_f a) = 0.168$). For small separation distances, a tensile normal stress occurs at the trailing edge when the fluid is Newtonian, while a larger tensile stress is observed for a second-order fluid. In figure 2(*b*), the particle is moving towards the wall. The stress is compressive at the leading edge for a Newtonian fluid whereas a large tensile stress is observed for a second-order fluid. This tensile stress arises from the modified pressure, $(\alpha_1/\mu_f)(\partial p_N/\partial t)$. If one calculates $T_n + p$ at this point, the result is zero because the shear rate is zero at this point. This is in agreement with the results by Joseph & Feng (1996). For a large separation distance, the last term in (3.1), which is related to the shear rate, and second term of the right-hand side of (3.1), which generates an extensional normal stress, are of the same order and relatively small compared to the overall force applied to the particle. For a particle nearly touching the wall, $(\alpha_1/\mu_f)(\mathrm{D}p_N/\mathrm{D}t)$ is much larger than $\frac{1}{4}\beta \mathrm{tr}\boldsymbol{A}^2$ and this results in a large deviation from the Newtonian case. The shear stress in a second-order fluid is similar to that in the Newtonian fluid when the separation distance is large. However, as the separation distance decreases, the shear stress differs from that of a Newtonian fluid because of the term $\alpha_1(\partial A/\partial t)$. The total force acting on the particle moving away from or towards the wall is plotted in figure 3(*a*). It can be observed that the contribution of the second-order fluid to the overall force applied to the particle is towards the wall independently of the direction of motion of the particle.

4. Motion of a particle very close to a wall

In this section, a perturbation method is used when De and $\epsilon = h/a - 1$ are small and there is no constraint on α_1 and α_2. The dimensionless stretched cylindrical coordinates are defined as $Z = z/a\epsilon$ and $R = r/a\sqrt{\epsilon}$. It can be shown that the dimensionless velocity and pressure are scaled as

$$\left.\begin{aligned} u_r^* &= \sqrt{\epsilon}\left[U_{1r}^* + \frac{De}{\epsilon}U_{2r}^* + \text{h.o.t.}\right], \quad u_z^* = U_{1z}^* + \frac{De}{\epsilon}U_{2z}^* + \text{h.o.t.}, \\ p^* &= \epsilon^{-2}\left[P_1^* + \frac{De}{\epsilon}P_2^* + \text{h.o.t.}\right] \end{aligned}\right\} \tag{4.1}$$

and De/ϵ is a small quantity compared to one. Superscript $*$ refers to dimensionless variables. The surface of the sphere is described by $Z = H = 1 + \frac{1}{2}R^2 + O(\epsilon)$. The terms

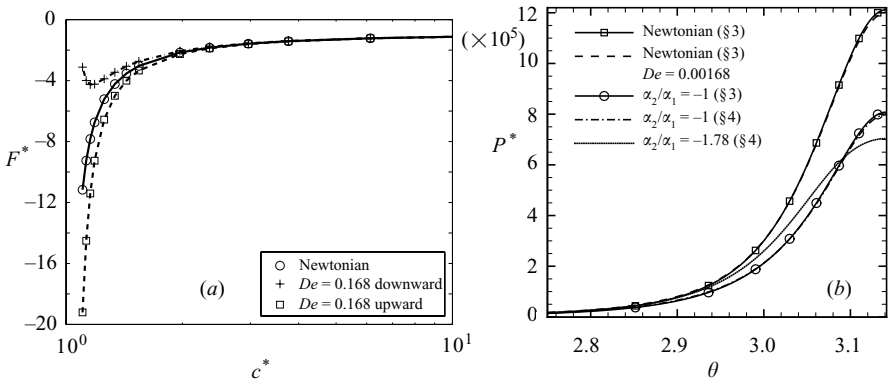

FIGURE 3. (*a*) Force $F^* = F/(6\pi\mu_f aU)$ acting on a spherical particle moving away from or towards the wall at $Re = 0.05$. (*b*) Dimensionless pressure for a sphere moving towards the wall at $Re = 0.05$ and $c^* = 1.01$.

U_{1r}^*, U_{1z}^*, and P_1^* are determined by Jeffrey & Corless (1988) as

$$U_{1r}^* = \frac{3R(Z^2 - HZ)}{H^3}, \quad U_{1z}^* = -\frac{2Z^3 - 3HZ^2}{H^3} + \frac{3R^2(Z^3 - HZ^2)}{H^4} \quad P_1^* = -\frac{3}{H^2}. \tag{4.2}$$

The solution at the first order of De can be determined using the following equations:

$$\left.\begin{aligned} \partial P_2^*/\partial Z &= -\partial\left(B_{1zz}^* + \frac{\alpha_2}{\alpha_1}A_{1zz}^{*2}\right)\Big/\partial Z \\ \partial P_2^*/\partial R &= -\frac{1}{R}\left[\partial R\left(B_{1rr}^* + \frac{\alpha_2}{\alpha_1}A_{1rr}^{*2}\right)\Big/\partial R\right] - \partial\left(B_{1rz}^* + \frac{\alpha_2}{\alpha_1}A_{1rz}^{*2}\right)\Big/\partial Z + \partial^2 U_{2r}^*/\partial Z^2 \end{aligned}\right\}$$

$$\partial(RU_{2r}^*)/\partial R + R\partial U_{2z}^*/\partial Z = 0 \tag{4.3}$$

where $\boldsymbol{B}_1^*$ is the dimensionless tensor $\boldsymbol{B}$ (defined in (2.3)) for velocity field $\boldsymbol{U}_1^*$. The boundary conditions to be applied are: $\mathbf{U}_2^*(Z=0) = \mathbf{U}_2^*(Z=H) = 0$. Since $\mathbf{u}^*$ is a function of R, Z, and ϵ, the term $\partial\mathbf{A}_1^*/\partial t^*\big|_{r,z}$ can be calculated as follows:

$$\left.\frac{\partial\mathbf{A}_1^*}{\partial t^*}\right|_{r,z} = -\frac{R}{2\epsilon}\left.\frac{\partial\mathbf{A}_1^*}{\partial R}\right|_{Z,\epsilon} - \frac{Z}{\epsilon}\left.\frac{\partial\mathbf{A}_1^*}{\partial Z}\right|_{R,\epsilon} + \left.\frac{\partial\mathbf{A}_1^*}{\partial\epsilon}\right|_{R,Z}. \tag{4.4}$$

Solving (4.3), U_{2r}^*, U_{2z}^*, and P_2^* can be determined. The dimensionless pressure is plotted in figure 3(*b*). As can be seen, the results from § 3 and this section are in agreement when $\alpha_1 + \alpha_2 = 0$, as expected. The difference between pressure in second-order and Newtonian fluids at the stagnation point is more pronounced as $|\alpha_2/\alpha_1|$ is increased. The pressure at the stagnation point can be written as

$$p|_{Z=H,R=0} = -3\frac{\mu_f U}{a}\left[\frac{1}{\epsilon^2} + \frac{De}{10\epsilon^3}\left(14 - 6\frac{\alpha_2}{\alpha_1}\right)\right]. \tag{4.5}$$

The total force acting on the particle can be written as

$$F^* = -\frac{1}{\epsilon}\left[1 + \frac{De}{10\epsilon^3}\left(2 - 3\frac{\alpha 2}{\alpha_1}\right)\right]. \tag{4.6}$$

Equation (4.6) is in agreement with the results shown in figure 3(*a*).

5. Viscoelastic potential flow

Irrotational normal stresses produced by potential flow of a second-order fluid give rise to motion of solid bodies which agrees with experimental observations as explained in the introduction. The shear stress and tangential velocity on the boundaries are in general discontinuous in viscous and viscoelastic irrotational flows. Potential flow of a viscous or viscoelastic liquid is incompatible with the no-slip condition at the boundary of the liquid and solid. However, to consider particle interaction in viscoelastic flow, we could look at viscoelastic potential flow locally. The literature shows that the sedimenting particles chain robustly in all flows: sedimentation, fluidization, shear flows, oscillating shear flows, and elongational flows. This chaining occurs for particles ranging in sizes from microns to centimeters (Joseph, Funada & Wang 2007). Therefore the cause must be local and we believe the local mechanism is due to the change in the normal stress which we compute in the second-order order fluid. Locally, near the stagnation point, the flow is slow and it could be argued that for this reason the local behaviour is second order. Takagi *et al.* (2003) similarly use the idea of a local Stokes flow at the boundary of a moving particle. In addition, at the stagnation point, the no-slip condition is satisfied exactly while the slip velocity is small in the vicinity of the stagnation point. This is a valid argument to look at the normal stresses in the neighbourhood of the stagnation point in a second-order fluid using viscoelastic potential flow.

It has been shown that for potential flow where $\mathbf{u} = \nabla\phi$ (Joseph 1992)

$$\nabla\cdot(\alpha_1\boldsymbol{B} + \alpha_2\boldsymbol{A}^2) = (3\alpha_1 + 2\alpha_2)\nabla\chi, \qquad \chi = \frac{\partial^2\phi}{\partial x_i\partial x_j}\frac{\partial^2\phi}{\partial x_i\partial x_j} = \frac{1}{4}\mathrm{tr}\boldsymbol{A}^2. \tag{5.1}$$

Thus, divergence of the stress is irrotational. Using (5.1), the pressure can be calculated using the Bernoulli equation. Thus, the stress tensor for viscoelastic potential flow can be written as

$$\boldsymbol{T} = \left[\rho\frac{\partial\phi}{\partial t} + \frac{1}{2}\rho|\nabla\phi|^2 - \beta\chi - C(t)\right]\boldsymbol{I} + \left[\mu_f + \alpha_1\left(\frac{\partial}{\partial t} + \boldsymbol{u}\cdot\nabla\right)\right]\boldsymbol{A} + (\alpha_1+\alpha_2)\boldsymbol{A}^2. \tag{5.2}$$

For a spherical particle moving perpendicularly to a wall as shown in figure 1, the potential flow solution can be obtained using the image of a doublet source in a sphere and is given as the series (Lamb 1945)

$$\phi = U\left(\frac{\mu_0\cos\gamma}{d^2} + \frac{\mu_1\cos\gamma_1}{d_1^2} + \frac{\mu_2\cos\gamma_2}{d_2^2} + \ldots\right) + U\left(\frac{\mu_0\cos\gamma'}{d'^2} + \frac{\mu_1\cos\gamma_1'}{d_1'^2} + \frac{\mu_2\cos\gamma_2'}{d_2'^2} + \ldots\right), \tag{5.3}$$

where $\mu_0 = \frac{1}{2}a^3$, a is the particle radius, U is the particle velocity, A is the center of a sphere moving towards the wall, B is the center of the imaginary sphere on the other side of the wall, $d = AP$, $d' = BP$, $d_1 = A_1P$, $d_1' = B_1P$, etc., are the distances between the doublets and a fixed point P. $AA_1 = f_1$, $AA_2 = f_2$, etc. can be defined using

$$\left.\begin{aligned} &f_1 = c - \frac{a^2}{c}, \quad f_2 = \frac{a^2}{f_1}, \quad \frac{\mu_1}{\mu_0} = -\frac{a^3}{c^3}, \quad \frac{\mu_2}{\mu_1} = -\frac{a^3}{f_1^3}, \\ &f_3 = c - \frac{a^2}{c-f_2}, \quad f_4 = \frac{a^2}{f_3}, \quad \frac{\mu_3}{\mu_2} = -\frac{a^3}{(c-f_2)^3}, \quad \frac{\mu_4}{\mu_3} = -\frac{a^3}{f_3^3}, \ldots, \end{aligned}\right\} \tag{5.4}$$

where c is twice the separation distance between the sphere and the wall. Using (5.3) and (5.4), we have

$$\phi = U\varphi(r, z, c) \Rightarrow \frac{\partial\phi}{\partial t} = a_c\varphi + 2U^2\frac{\partial\varphi}{\partial c}, \tag{5.5}$$

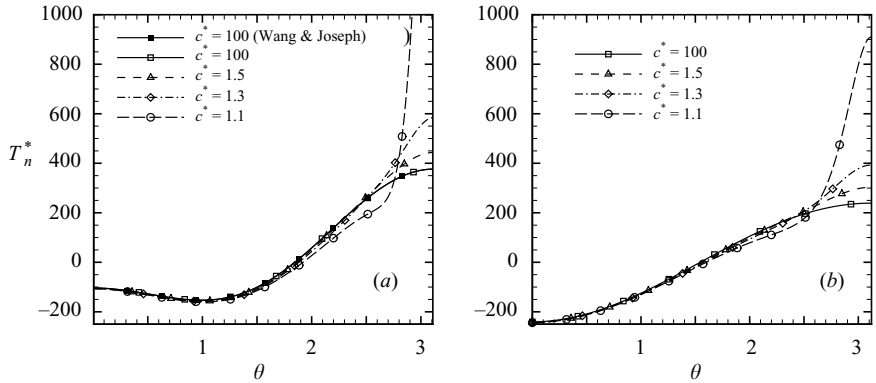

FIGURE 4. A spherical particle moving away from the wall at $Re = 0.05$, $De = 0.168$, and $\alpha_2/\alpha_1 = -1.78$ (*a*) Second-order fluid, (*b*) Newtonian fluid.

where a_c is the sphere acceleration. Also,

$$\boldsymbol{A} = U\tilde{\boldsymbol{A}} = 2U \begin{pmatrix} \dfrac{\partial^2\varphi}{\partial r^2} & \dfrac{\partial^2\varphi}{\partial r\partial z} & 0 \\ \dfrac{\partial^2\varphi}{\partial r\partial z} & \dfrac{\partial^2\varphi}{\partial z^2} & 0 \\ 0 & 0 & \dfrac{1}{r}\dfrac{\partial\varphi}{\partial r} \end{pmatrix}. \tag{5.6}$$

Thus, the stress tensor can be written as

$$\begin{aligned} \boldsymbol{T} + C\boldsymbol{I} = \mu_f\tilde{\boldsymbol{A}}U + (\rho\varphi\boldsymbol{I} + \alpha_1\tilde{\boldsymbol{A}})a_c + \Bigg(\Bigg[2\rho\frac{\partial\varphi}{\partial c} + \frac{1}{2}\rho\left\{\left(\frac{\partial\varphi}{\partial r}\right)^2 + \left(\frac{\partial\varphi}{\partial z}\right)^2\right\} \\ - \beta\left\{\left(\frac{\partial^2\varphi}{\partial r^2}\right)^2 + \left(\frac{1}{r}\frac{\partial\varphi}{\partial r}\right)^2 + \left(\frac{\partial^2\varphi}{\partial z^2}\right)^2 + 2\left(\frac{\partial^2\varphi}{\partial r\partial z}\right)^2\right\}\Bigg]\boldsymbol{I} \\ + 2\alpha_1\frac{\partial\tilde{\boldsymbol{A}}}{\partial c} + \alpha_1\tilde{\boldsymbol{u}}\cdot\nabla\tilde{\boldsymbol{A}} + (\alpha_1+\alpha_2)\tilde{\boldsymbol{A}}^2\Bigg)U^2. \end{aligned} \tag{5.7}$$

The normal stress T_n and the shear stress T_t are

$$T_n = T_{rr}\sin^2\theta + T_{zz}\cos^2\theta + T_{rz}\sin 2\theta \quad T_t = \frac{T_{rr} - T_{zz}}{2}\sin 2\theta + T_{rz}\cos 2\theta. \tag{5.8}$$

Using (5.3), (5.7) and (5.8), the normal stress is computed at the surface of a sphere moving with constant velocity U perpendicularly to the wall. Figure 4 shows the dimensionless normal stress as a function of θ for different separation distances when the particle is moving away from the wall for $Re = 0.05$ and $De = 0.168$ which agree with the published results by Wang & Joseph (2004) when $c \to \infty$. It can be seen that for small separation distances, a tensile normal stress occurs at the trailing edge when the fluid is Newtonian, while a larger tensile stress is observed for a second-order fluid. In figure 5, the particle is moving towards the wall. The stress is compressive at the leading edge for a Newtonian fluid whereas a large tensile stress is observed for a second-order fluid. This behaviour can be explained by examination of (5.7). The first term is the same for Newtonian and second-order fluids while for a non-accelerating particle, the second term is zero. The third term, which strongly depends on viscoelasticity, is proportional to U^2 and is independent of the direction of motion. Thus, a tensile stress is observed on the sphere surface at $\theta = \pi$

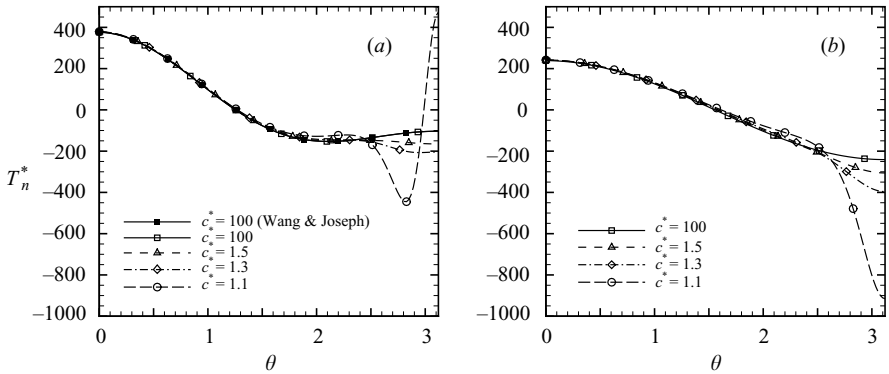

FIGURE 5. A spherical particle moving towards the wall at $Re = 0.05$, $De = 0.168$, and $\alpha_2/\alpha_1 = -1.78$ (*a*) Second-order fluid, (*b*) Newtonian fluid.

in both cases when the particle is moving away from or towards the wall. The Stokes and potential flows give different but complementary results when the motion is steady, due to the shear rate and extensional normal stresses, respectively. For unsteady flows, the Stokes flow evaluation of the stresses also gives rise to tension at a point of stagnation.

6. Conclusions

The force predicted by Stokes equations for a spherical particle moving perpendicularly to a wall in a second-order fluid with $\alpha_1 + \alpha_2 = 0$ is calculated and it is shown that the contribution of the second-order fluid to this force is independent of the direction of motion of the particle and it is always an attractive force towards the wall. The perturbation method for the case with non-zero $\alpha_1 + \alpha_2$ small De for a sphere very close to a wall is utilized. The difference between the normal stress of second-order and Newtonian fluids at the stagnation point is more pronounced as $|\alpha_2/\alpha_1|$ is increased. Moreover, the viscoelastic potential flow for a spherical particle moving normal to a wall is obtained for a second-order fluid and the results are compared with those predicted by a Stokes analysis and a perturbation method.

The first author thanks Mr. Sadegh Dabiri for valuable discussions.

REFERENCES

ARDEKANI, A. M. & RANGEL, R. H. 2006 Unsteady motion of two solid spheres in Stokes flow. *Phys. Fluids* **18**, 103306.

ARDEKANI, A. M. & RANGEL, R. H. 2007 Numerical investigation of particle–particle and particle–wall collisions in a viscous fluid. *J. Fluid Mech.* (submitted).

BATCHELOR, G. K. & GREEN, J. T. 1972 The determination of the bulk stress in a suspension of spherical particles to order c2. *J. Fluid Mech.* **56**, 401–427.

BECKER, D. L. E., MCKINLEY, G. H. & STONE, H. A. 1996 Sedimentation of a sphere near a plane wall: Weak non-Newtonian and inertial effects. *J. Non-Newtonian Fluid Mech.* **63**, 45–86.

BIRD, R., ARMSTRONG, R. & HASSAGER, O. 1987 *Dynamics of Polymeric Liquids*. John Wiley.

BRENNER, H. 1961 The slow motion of a sphere through a viscous fluid towards a plane surface. *Chem. Eng. Sci.* **16**, 242.

BRINDLEY, G., DAVIES, J. M. & WALTERS, K. 1976 Elastico-viscous squeeze films. Part I. *J. Non-Newtonian Fluid Mech.* **1**, 19–37.

BRUNN, P. 1977 Interaction of spheres in a viscoelastic fluid. *Rheologica Acta* **16**, 461–475.

COLEMAN, B. & NOLL, W. 1960 An approximation theorem for functionals, with applications in continum mechanics. *Arch. Rat. Mech. Anal.* **6**, 355–370.

Davis, R. H. 1987 Elastohydrodynamic collisions of particles. *PhysicoChem. Hydrodyn.* **9**, 41–52.

Engmann, J., Servais, C. & Burbidge, A. S. 2005 Squeeze flow theory and applications to rheometry: A review. *J. Non-Newtonian Fluid Mech.* **132**, 1–27.

Fortes, A. F., Joseph, D. D. & Lundgren, T. S. 1987 Nonlinear mechanics of fluidization of beds of spherical particles. *J. Fluid Mech.* **177**, 467–483.

Goldman, A. J., Cox, R. G. & Brenner, H. 1967 Slow viscous motion of a sphere parallel to a plane wall. I. Motion through quiescent fluid. *Chem. Engng. Sci.* **22**, 637–651.

Ho, B. P. & Leal, L. G. 1976 Migration of rigid spheres in a two-dimensional unidirectional shear flow of a second-order fluid. *J. Fluid Mech.* **79**, 783–799.

Jeffrey, D. J. 1973 Conduction through a random suspension of spheres. *Proc. R. Soc. Lond.* A **335**, 355.

Jeffrey, D. J. & Corless, R. M. 1988 Forces and stresslets for the axisymmetric motion of nearly touching unequal spheres. *PhysicoChemHydrodyn.* **10**, 461.

Joseph, D. D. 1990 *Dynamics of Viscoelastic Liquids*. Springer.

Joseph, D. D. 1992 Bernoulli equation and the competition of elastic and inertial pressure in the potential flow of a second-order fluid. *J. Non-Newtonian Fluid Mech.* **42**, 358–389.

Joseph, D. D. & Feng, J. 1996 A note on the forces that move particles in a second-order fluid. *J. Non-Newtonian Fluid Mech.* **64**, 299–302.

Joseph, D. D., Funada, T. & Wang, J. 2007 *Potential Flows of Viscous and Viscoelastic Fluids*. Cambridge University Press.

Joseph, D. D., Liu, Y. J., Poletto, & M. Feng, J. 1994 Aggregation and dispersion of a spheres falling in viscoelastic liquids. *J. Non-Newtonian Fluid Mech.* **54**, 45–86.

Joseph, G. G., Zenit, R., Hunt, M. L. & Rosenwinkel, A. M. 2001 Particle-wall collisions in a viscous fluid. *J. Fluid Mech.* **433**, 329–346.

Koch, D. L. & Subramanian 2006 The stress in a dilute suspension of spheres suspended in a second-order fluid subject to a linear velocity field. *J. Non-Newtonian Fluid Mech.* **138**, 87.

Lamb, H. 1945 *Hydrodynamics*. Dover.

Leal, L. G. 1975 The slow motion of slender rod-like particles in a second-order fluid. *J. Fluid Mech.* **69**, 305–337.

Liu, Y. J. & Joseph, D. D. 1993 Sedimentation of particles in polymer-solutions. *J. Fluid Mech.* **255**, 565–595.

Maude, A. D. 1961 End effects in a falling-sphere viscometer. *Br. J. Appl. Phys.* **12**, 293.

Mifflin, R. T. 1985 Dissipation in a dilute suspension of spheres in a second-order fluid. *J. Non-Newtonian Fluid Mech.* **17**, 267–274.

Pasol, L., Chaoui, M., Yahiaoui, S. & Feuillebois, F. 2005 Analytic solution for a spherical particle near a wall in axisymmetrical polynomial creeping flows. *Phys. Fluids* **17**, 073602.

Riddle, M. J., Narvaez, C. & Bird, R. B. 1977 Interactions between two spheres falling along their line of centers in viscoelastic fluid. *J. Non-Newtonian Fluid Mech.* **2**, 23–25.

Rivlin, R. S. & Ericksen, J. L. 1955 Stress deformation relations for isotropic materials. *J. Rat. Mech. Anal.* **4**, 323–425.

Rodin, G. 1995 Squeeze film between two spheres in a power-law fluid. *J. Non-Newtonian Fluid Mech.* **63**, 141–152.

Singh, P. & Joseph, D. D. 2000 Sedimentation of a sphere near a wall in Oldroyd-B fluid. *J. Non-Newtonian Fluid Mech.* **94**, 179–203.

Sun, K. & Jayaraman, K. 1984 Bulk rheology of dilute suspensions in viscoelastic liquids. *Rheol. Acta* **23**, 84.

Takagi, S., Oguz, H. N., Zhang, Z. & Prosperetti, A. 2003 A new method for particle simulation - part ii: Two-dimensional Navier-Stokes flow around cylinders. *J. Comput. Phys.* **187**, 371–390.

Tanner, R. I. 1985 *Engineering Rheology*. Clarendon.

Wang, J. & Joseph, D. D. 2004 Potential flow of a second-order fluid over a sphere or an eclipse. *J. Fluid Mech.* **511**, 201–215.